Characterization of vertical profile of rain micro-structure using Micro Rain Radar in a tropical part of Nigeria

[1]A. C. Tomiwa*, [2]J. S. Ojo and [3]M. O. Ajewole
[1]Department of Physics and Electronics, AdekunleAjasin University, AkungbaAkoko, Ondo State, Nigeria
E-mail: tomiwaakinyemiclem@gmail.com*; akinyemi.tomiwa@aaua.edu.ng*
[2, 3]Department of Physics, Federal University of Technology, Akure, P.M.B. 704, Akure, Ondo State Nigeria.
E-mail:josnno@yahoo.com; oludareajewole61@yahoo.com

Abstract

Understanding the vertical microstructure of rain is one of the key tools to the physical processes of rain attenuation. In this paper, one-year(January 2010- December, 2010) data of rainfall parameters were considered and the microstructure of rain were studied using a vertically-pointing Micro Rain Radar (MRR) located at The Federal University of Technology Akure, Nigeria. Rainfall parameters were measured from the ground level to a height of 4.8 km above sea level with a vertical resolution of 0.16 km. The rain rates were classified into low (stratiform) and high (convective). These classifications were based on different profile rain microstructure, among which are rain rates, liquid water content, Drop Size Distribution (DSD), average fall speed of the drops and radar reflectivity. The results show that the rain height obtained from the bright band's signature of melting layer of radar reflectivity profile vary between the heights 4.0 km and 4.3 km (equivalent to 4.36 and 4.66 km above sea level) as compared to the fixed value of 4.86 km assigned by the International Telecommunication Union-Recommendations (ITU-R) 839-4. DSD distribution is also narrow when the rain rate is low and becomes significantly wider with increasing rain rate, indicating the increasing presence of larger drops. Comparison of rain rate measurement made by the ground based rain gauge and from the 160 m level obtained from MRR shows some level of agreement at smaller rain rate values. The overall results could lead to better understanding of microstructure of rain needed for analysis of rain attenuation study in this region.

Keywords*:* Rain microstructure; Stratiform; Convective rain; Micro Rain Radar; Bright band signature; Tropical region

* *Corresponding author*

1 Introduction

Water plays a prominent role in the atmosphere and is the most dominant impairment for the propagation of radio waves (Das et al., 2010). Rain water may seriously affect the performance of microwave links operating at frequencies greater than 10 GHz (Karmakar*et al*., 2011, Ojo and Omotosho, 2013). It is of great interest to measure atmospheric water in all its

phases. In its gaseous phase it occurs as water vapor, in liquid form as cloud liquid water, drizzle or rain and in its solid form as cloud ice, dry snow or hail (Matlizer, 2009). As many forms of appearance exist, many properties have to be considered. This is a great challenge for the measurement technique.

Melting snow strongly interacts with microwave radiation, whereas the interaction with rain is relatively weaker and the interaction with dry snow is negligible (Fabry and Zawadzki, 1995). The region of melting snow is called the melting layer. This is the layer below the 0^{o}C isotherm height down to the height where the falling particles have the shape of the rain drops. Rain attenuation models are estimated based on rain drops, which depend on the rain height. The ITU-R generalized the rain height with constant value derived from the zero degree isotherm height with a uniform vertical rain structure (ITU. R P. 839-4, 2013). These assumptions have been found not to be true for the tropical regions (Ajayi and Barbaliscia, 1990, Das *et al*., 2010). The tropical region is known to be characterized by very heavy rainfall which is sometimes accompanied by thunderstorms (Ojo *et al*., 2009) when compared with temperate counterparts.

The country itself has two distinct seasons: Wet (March-October) and dry (November-February of the following year). The average rainfall in a location depends on the movement of the Inter-tropical Discontinuity (ITD). Heavy rainfall usually occurs during the wet season in this location and during this period, the ITD moves across the country. Rainfall in this location can be classified into: Stratiform and convective rainfall. Stratiform precipitation results from formation of small ice particles joined together to form bigger nuclei. The growing nuclei become unstable and as they pass through the so-called melting layer, (extending from about 0.5 to 1 km below the 0^{o}C isotherm) they turn into raindrops that fall down to the earth's surface, with a horizontal extent of hundreds of kilometres for durations exceeding an hour. The convective precipitation on the other hand is associated with clouds that are formed in general below the 0^{o}C isotherm and are stirred up by the strong movement of air masses caused by differences in tropospheric pressure. In this process, water drops are created and grow in size, until they fall to the earth's surface. The horizontal scale is of several kilometres for durations of tens of minutes (Ajayi and Olsen, 1985).

Several works on profile investigation of microstructures of rainfall have been reported in the temperate region by several researchers (Peter *et al*., 2006, Clemens et al., 2006, Ojo *et al.,* 2013) using Disdrometer, Doppler radar, and a Micro Rain Radar (MRR) among others but there is still little or no observations in the tropical region, especially Nigeria. As Nigeria is planning to launch another communication satellite with transponders for Ku/Ka and V-bands, there is a need to investigate the vertical rain structure for different rain types that can mitigate the propagation of signals at these frequency bands in this region.

2. Some theoretical concepts

The MRR used in this work is a profiling Frequency Modulated Continuous Wave (FM-CW) Doppler radar, which operates at a frequency of 24.1 GHz. It measures the backscattered signal from the rain drops to calculate different microphysical parameters at different heights. The measured Doppler spectra are converted into drop diameters to provide Information on the DSD using different known relationships. Explicit descriptions of different microphysical parameters have been provided in the works of Das *et al*., (2010), Strauch, 1976, Peter *et al*, 2002)among others. Rain microstructure R, LWC and radar reflectivity (Z) are estimated from the DSD, while the V_m is calculated from the measured Doppler spectrum.

Following the works of Waldvogel, (1974), Peter et al. (2002), Peter *et al*. (2006), Clemens et al. (2006) and Marzuki*et al*. (2016)the integral parameters from the DSD are expressed for each of the rain microstructures as:

$$R = \frac{6\pi}{10^4}\int_0^\infty D^3 N(D) v(D) dD \quad (1)$$

$$Z = \int_0^\infty N(D)\, D^6 dD \quad (2)$$

$$LWC = \frac{\pi}{6}\rho_w \int_0^\infty N(D) D^3 dD \quad (3)$$

$$D_m = \int_0^\infty \frac{N(D) D dD}{N(D) dD} \quad (4)$$

where R is the rain rate in mm/h, Z is the radar reflectivity in dBZ, LWC is the liquid water content in mg/m^3, D_m is the mean drop diameter (mass-weighted mean diameter) in mm(Das *et al.*, 2010), $N(D)$ is the number of drops per unit volume with the size D to $D + \Delta D$ in mm^{-1}m^{-3}, D is the diameter of the drops in mm, $v(D)$ is the fall velocity of the drops with size D to $D + \Delta D$ in m/s, ρ_w is the density of water.

The mass-weighted mean diameter D_m is also related to the coefficient No and the total drop concentration N_T as (Steiner and Smith, 2004):

$$No = \frac{(4+\mu)^{(1+\mu)}}{\Gamma(1+\mu)} \frac{N_T}{(D_m)^{(1+\mu)^2}} \quad (5)$$

whereμ is the raindrop size distribution shape factor and Γ is a gamma function in the expression.

Many works have been performed relating the rainfall rate R, and Z leading to a general expression of the form (Peter *et al*. 2006):

$$Z = {}^{a}R^{b} \tag{6}$$

where Z is given in mm^6m^{-3}, R in mmh^{-1}, a and b are coefficients which depend on the raindrop number distribution $N(D)$ as function of the drops diameter (D).

Equation (6) was used to determine the relationship between rainfall rate (R) and radar reflectivity factor (Z). Natural logarithm is applied to both sides of Equation (6) resulting in (Samento *et al.,* 2006):

$$\text{Ln } Z = \text{Ln } a + b \text{ Ln } R \tag{7}$$

The coefficients a and b of equation (6) were estimated by linear regression Z versus R.

The average fall velocity V_m obtained from the measured Doppler spectrum follows the form(Peter *et al.*, 2002):

$$v_m = \frac{\lambda}{2} \frac{\int_0^\infty f.P(f)df}{\int_0^\infty P(f)df} \tag{8}$$

whereλ is the wavelength, f is the Doppler frequency in Hz and p(f) is the spectral Doppler power as related to Doppler frequency. Equation (6) is related to DSD weighted by D^6 as (Peter et al., 2002):

$$v_m = \frac{\int_0^\infty N(D)D^6 v(D)dD}{\int_0^\infty N(D)D^6 dD} \tag{9}$$

3. Project site and Data analysis

The experimental site is the Federal University of Technology, Akure (7˚15'N, 5° 15'E), located in the Southwestern part of Nigeria. The map of the measuring site is as shown in Figure 1. The altitude above the sea level of the location is 358 m. The vertical profiles of rain parameters were observed using an MRR. It has an instantaneous measurement at every 10 s integrated over 1-min with a vertical resolution of 160 m. The 160 m resolution is taken to accommodate the nearly complete profile of the rain up to 4.8 km over this region with a total of 30 range gates. The altitude to the sea level of the location is also taken into consideration in the final estimation of the rain height level.

The MRR generates a height range resolved Doppler spectrum. The data processing is performed by a Radar Control and Processing Device (RCPD) which is placed in housing directly below the antenna support. The measured data are transmitted by a serial RS-232 port rate from the outdoor unit. This port connects the MRR to a Personal computer; hence the

control, the calculation of further values, and the recording of the data can be done with the MRR-control program.

The DSD is calculated for drop diameters from 0.246 to 5.04 mm with falling velocities from 0.88 to 9.14 m/s. Rain type is identified based on the presence/absence of bright band's signature. The rain is identified as stratiform when the profile shows the bright band's signature while the convective type of rain is identified by the absence of any bright band (Fabry and Zawadzki, 1995, Klaassen, 1988, Awaka *et al*., 1998, Rao *et al*., 2001, Kunhikrishnan *et al*, 2006, Cha *et al*, 2007, Das *et al*., 2010). A detailed description of the classification scheme of these rain types is available in the work of Das *et al.*(2010). Any possible error that may arise from the possibility of misidentification of bright band and which may lead to improper classification of rain were minimized by taking a continuous measurement so that in any random peak is removed in larger sets. Although, one of the major problems of MRR is its higher frequency of operation (24 GHz), the signals get attenuated in heavy rain, which limits the analysis of light-moderate rain. Before processing the MRR data for this study, appropriate attenuation correction for moderately high rain rates is done by calculating the Mie extinction from the derived DSD using the method adopted on the work of Peter *et al*., (2002). It has been established that in the Mie scattering region, the size of the scattering particle and the wavelength of the incident radiation are comparable (raindrops typically have diameters in the range 0.2-6 mm); hence the resultant cross sections are relatively insensitive to the size of the raindrops (Joss and Gori, 1978, Maitra and Gibbins, 1995). This procedure was used to cater for the attenuation correction due to higher frequency of the MRR.

4. Observations from the measurement

The present study is based on the preliminary results of vertical profile of rain observed using a vertically pointing MRR at Akure, Nigeria ($7^{o}15$'N, $5^{o}15$'E) during the intense rainfall (rainy days during one of the wet months of the year 2010). Rain microstructure of mean DSD, rain rate (R), liquid water content (LWC) and Doppler velocity of drops, V_m (which includes fall velocity and the ambient vertical air motion) were analyzed based on rain types in order to obtain better understanding of rain attenuation study. A further comparison of rain rate characteristics was also made with the one obtained from the ground based raingauge in order to give an insight into the extent of applicability of ground measurements for rain attenuation prediction over an Earth-space link.

In order to present the general overview of all the rain measured during the period under study, Table 1 shows the comparison of rain events that were captured in the data over the study period and the respective total time for which the threshold values were exceeded. The values in the bracket represent the total rain accumulation that contributed to the rain duration for the

period of study. In general, the total monthly (annual) rain accumulation for the period of study is about 11,823 mm, which comprises about 344 mm for the dry months and 11, 479 mm for the wet months. Also, the estimated LWC for the overall event and rain type and for all the heights considered was about 86.76 mgm^{-3}. Further observation from the Table indicates that the rain rate $0< R \leq 5$ categorized as drizzle contributed most of the rain events in this region followed by rain rate$5< R <10$ (widespread) and then rain rate greater than 40 mm/h categorized as thunderstorm rain type contributed least with about 291 total events. Analyzing the event period further shows that the stratiform rain which is characterized by medium and low intensities is in long duration while the stormy showers with high rain rates as a result of convective type of rain occur for a short period. For the purpose of this report, we initially examined the vertical structure of reflectivity from the MRR measurements at different rain events. Comparison of the rain rate was also made on the observation from MRR at 160 m level with measurements taken by a rain gauge in order to validate the MRR measurement.

The MRR measurements during the year 2010 are characterized by the occurrence of several events with quite some significant bright band signature. Typical results of such events are presented in Figs 1 (a-b) for different days and time span. For the typical rain events observed on 26th October 2010 between 16:20 and 17:15 GMT LT and 31st October 2010 between 03:40 and 04:50 GMT LT, the maximum *R* for the observed period (1h 55 min) is about 10.04 mm/h. Results from Figs 1 (a and b) clearly show that whenever there is bright band, the rain rate at lower heights has low values as real evidence of stratiform condition. Also, when the radar bright band is absent, the *R* at lower heights are found to be high in the present spectrum, which could be categorized as convective rain (Cha *et al*., 2007, Das *et al*., 2010). This is just an assumption anyway, since some shallow rain or the weak rain without a detectable bright band (with MRR) can have a smaller rain rate. Further study may be needed to justify the claim.

4.1. ***Rain with bright and clear band***

The vertical profile of radar reflectivity as indicated in Fig. 1(a) shows the presence of bright band during the rain event between 4.1 and 4.4 km above the ground level. It could further be observed that bright band was clearly observed around 16.20 GMT LT while partial one was observed at 16.31 GMT LT. However, around 17.00 GMT LT there is no evidence of bright band. These show the complete transformation from stratiform to mixed and convective rain type respectively (Das *et al*., 2010).

The vertical profiles of different rain parameters, as given by MRR are presented in Fig 1b on 31st October 2010 from 03:40 to 04:50 GMT LT. There is also a similar type of structures found around 4.10–4.18 GMT LT with clear evidence of bright band. Partial occurrence of bright band could also be observed at some later time of the day. The convective nature of the rain type due

to non-bright band observed in some of the time of the day referred to here may only be assumed to be a case of weakness in magnitude and may not necessarily be due to convective rain type.

4.2. Micro Rain Radar Observation

Figures 2a - 2d present the vertical profiles of different rain parameters obtained by MRR during the rain event on 26thOctober, 2010. For example, in Fig 2 (a), the vertical profile of radar reflectivity is presented for 16:55-17:20 GMT LT, which depicts that there is bright band and the rain rate during this period is small, indicating not actually convective type but weak in magnitude as reported by Das *et al*. (2010). Other rainfall parameters are also presented in Figs 2b-2d. The profile of rain rate (Fig. 2b) follows the same pattern with that of liquid water content (Fig. 2c) with a peak around 2.8 km. However, a slight decrease is observed in the average fall velocity with a small enlargement near 4.2 km as indicated in Fig. 2 (d). Although not shown here for paucity of space sake, the same trend could be seen on the 31st October 2010 but with different peak at different heights.

Figures 3a- 3d also present the vertical profiles of different rain parameters as obtained from MRR during the rain event on 26th October, 2010 from 16:20 and 16:30 LT. The radar reflectivity profile indicates a clear cut zenith at 4.3 km that corresponds to the melting layer as shown in Fig. 3 (a). As earlier reported in section 1, the bright band is the evidence of the occurrence of stratiform rain. It is also noted that around the same height, rain rate increases (Fig. 3b). However, an increase in radar reflectivity is not an indication of increase in rain rate for the noted zenith rather the peak observed around 4.3 km is due to melting layer. The graph of vertical profiles of liquid water content also has a peak around the same height of 4.3 km as presented in Fig. 3 (c). However, the vertical profile of average fall velocity shows a small enlargement near 4.2 km. This is in agreement with observations from the work of Peter *et al*. (2002) and the recent work of Das *et al*. (2010). Although not the same values as obtained in this report, both papers observed that the average fall velocity appears at a certain peak due to melting layer. In overall, the results show that the rain height obtained from the bright band's signature of melting layer of radar reflectivity profile vary between the heights 4.0 km and 4.3 km (equivalent to 4.36 and 4.66 km above sea level) as compared to the fixed value of 4.86 km assigned by the ITU-R 839-4. The implication is that, the rain attenuation estimated using the predicted ITU value will be overestimated in this region, hence a local value of the rain height is recommended to achieve a better rain attenuation estimate needed for optimum system designing in this region.

Figures 4 (a) and (b) show typical rain DSD spectra based on the lognormal curves for all the rain types observed on the 26th October 2010 at 160 m and 640 m respectively. The distribution is narrow when the rain rate is low and becomes significantly wider with increasing rain rate, indicating the increasing presence of larger drops. The increasing trend of the number

of drops with drop diameter becomes more conspicuous as it moves from low diameter end to larger diameter of rain drops. The present study is not to determine whether the number of drops actually increases with drop diameter in this region since we have data only from 0.246 mm onwards. However, this can be clearly seen in the case of DSDs corresponding to large rain rates. Therefore, it may be reasonable to assume that this trend extends to the low rain rates also. Though, there is a possibility of underestimation in the number of smaller drops in heavy rains due to instrument's electronic design among other factors. Also, the number of smaller drops generally decreases with increasing rain rate due to the drop growth (collision and coalescence) and evaporation. In addition, the behavior of rain DSD at different rain types is very clear from visual observations of these spectra. For example, at $0.2<R\leq 1$ rain rate interval, an increase is seen in the drop diameter at which the distribution peaks with rain rate. The amplitude of this peak decreases as the rain rate increases. The behavior is very similar at 640 m, but with lower drop diameters for all the rain rates when compared with 320 m height. Similar trend could also be found in all the remaining height (not shown here due to paucity of space) although with the different drop diameter and the number of the drops.

Table 2 shows the comparison between Z-R relations obtained at different rain types over some heights at the tropical stations, Akure (present study) and Ile-Ife [22], with those obtained by Joss and Gori (1978), Marshall and Palmer (1948), Fujiwara (1965) and Jones (1956) for temperate stations. The Z and R are measured simultaneously but as a different variables by radar (Z) using the MRR based on the computation from computed using the $N(D)$ distributions as pointed out in equations (1) and (2). The coefficients a and b of the equation (6) were estimated by linear regression Z versus R. The same procedure was also adopted to obtain the prefactors, a and the exponent, b as presented in Table 3.

Table 3 also shows the comparison between M-R relations obtained at different rain types over some heights at the tropical stations, Akure and Ile-Ife (Ajayi and Olsen, 1985), with those obtained by Marshall and Palmer (1948), Jones (1956), Sekhon and Srivastava (1971) and Mueller (1960)for temperate stations. The most striking results from the two tables are the diversity of the Z-R and M-R coefficients fitted over this single dataset. For example, in the Z-R relations, the prefactor takes values in the range 213 up to 316; 190 up to 313; 172 up to 312 for drizzle, widespread and shower rain types respectively, while the exponents are in the range of 1.15 up to 1.35; 1.02 up to 1.19 and 1.07 up to 1.1 for drizzle, widespread and shower rain types respectively. Only a prefactor of 380 and an exponent of 1.55 is fitted for thunderstorm rain type due to insufficient data from other heights considered in this study. Similar trend could be observed in the M-R relation (Table 3) although with different prefactors and exponents, where M replaces the LWC. The Z-R also show a good quality of fit for the relations with correlation coefficients comprised between 0.53 – 0.86.

The Comparison was also made between the measurement made by MRR at height 160 m and ground based rain gauge. This will provide a better understanding of the results and to validate the reading from MRR. Fig. 5 (a) shows a good agreement between the actual rain rate measured both by MRR and rain gauge. The correlation coefficient between the two measurements is around 0.9 as presented in Fig. 5 (b). However, more measurements are needed to ascertain degree of the correlation.

5. CONCLUSION

Vertical profiles of rain microstructures, such as rain rate, drop size; liquid water content and average fall velocity have been analyzed for different rain types based on the propagation point of view. Using a MRR and ground based rain gauge, some case studies of tropical rain over the southwestern part of Nigeria, Akure are presented. From the MRR observation, rain is classified into two different types based on the different microphysical parameters mentioned above. The observation shows that the nature of rain changes with time during a rain event. The bright band due to the melting layer is noticed at around 4.3 km but is found to be sometime variable. The drop size distribution at different height gives an insight of the physical process associated with rain. A further comparison of rain rates with MRR and rain gauge on a typical event shows good agreement. Results from the analyses will provide a further insight into the tropical rain structure, and the applicability for satellite communication links designing at high frequencies for tropical sites.

Acknowledgement

Authors are grateful to Alexander von Humboldt Foundation and the Meteorological Institute, University of Bonn, Germany for providing MRR to the Department of Physics, FUTA, Nigeria.

REFERENCES

Ajayi G. O. and R. L. Olsen (1985): "Modeling of raindrop size distribution for microwave and millimeter wave applications," *Radio Sci.*, vol. 20, pp. 193–202, Mar.-Apr. 1985.

Ajayi G.O., and Barbaliscia, F (1990): Prediction of attenuation due to rain: characteristics of the 0^o isotherm in temperate and tropical climates, Int. J. Satellite Commun, 8, 187-196.

Awaka, J Iguchi, T and Okomoko, K (1998): Early results on rain type classification by the tropical rainfall measuring mission (TRMM) precipitation radar, in: proceedings of the eight URSI Commission F Open Sysposium, Averio, Portugal, PP. 143-146.

Cha, Joo-Wan, Seong, Soo Yum, Chang, Ki-Ho, Sung, Nam Oh (2007): Estimation of the melting layer from a Micro Rain Radar (MRR) data at the Cloud Physics Observation System (CPOS) site at Daegwallyeong Weather Station. APJAS 43 (1), 77–85.

Clemens M, Peters, G Seltman, J., and Winker, P (2006): Time-height evolution of measured raindrop size distribution, in: proceedings of the ERAD.

Das, S.,Ashish. K and Maitra A (2010): Investigation of vertical profile of rain microstructure at Ahmedabad in Indian tropical region, Advances in Space Research, 45, 1235-1243.

Fabry, F. Zawadzki., I (1995): Long-term radar observations of melting layer of precipitation and their interpretation. Journal of Atmos. Sci. 52, 838-851.

Fujiwara M (1965): Raindrop size distribution from individual storms, Journal of atmospheric Sciences, Vol. 23, 585-591.

International Telecommunication Union Recommendation 839-4, Rain height model for the prediction methods, (ITUR, Geneva, Switzerland), 2013.

Jones M.A Douglas (1956) Raindrop size distribution and Radar reflectivity, Illinois State Water Survey Meteorological Laboratory, 1- 20.

Joss J. and Gori E.G., 1978: Shapes of raindrop size distributions. J. Appl. Meteorol, 17, 1054-1061.

Karmakar P.K, Maiti M, Bhattacharyya K, Angelis C.F and Machado L.A.T (2011): Rain attenuation studies in the microwave band over southern latitude, *The Pacific J Sci Tech*, *(Hawaii)* 12, 196-205.

Klaassen, W (1988): Radar observations and simulation of the melting layer of precipitation, Journal of Atmos. Sci., 45, 3741-3753.

Kunhikrishnan, P.K., Sivaraman, B.R., Kumar, N.V.P.K. and Alappattu, D.P (2006): Rain observations with Micro Rain Radar (MRR) over Thumba, in: Proceedings of the SPIE, 6408 (64080L-1), 2006.

Maitra A, and Gibbins C.J (1995): Inference of raindrops size distribution from measurements of rainfall rate and attenuation at infrared wavelengths. Radio Science, Vol. 30 (4), 931-941.

Marshall, J.S. and W.M. Palmer (1948): "The distribution of raindrops with size", J. Meteorol. **5**, 165.

Marzuki, Hiroyuki H, Toyoshi S, Indah R, Mutya V, and Afdal (2016): Performance Evaluation of Micro Rain Radar over Sumatra through Comparison with Disdrometer and Wind Profiler, Progress In Electromagnetics Research M, Vol. 50, 33–46.

Matlizer (2009): Precipitation measurements with microwave sensors, Universiti Bern, Institute fur AngewandtePhysik, pp 1-2, 35-36.

Mueller E.A (1960): Study on the intensity of surface precipitation using Radar instrumentation. Quarterly technical report, No. 10, Illinois State Water Survey Urbana Illinois.

OjoJ.S,Ajewole M.O and EmilianiL.D(2009)**: "**Development of 1-minute rain rate contour maps for radio communication over Nigeria,"IEEE Ant. &propag. Magazine, Vol, 5 1, (5), 82-89

OjoJ.S and OmotoshoT.V (2013): Comparison of 1-minute rain rate derived from TRMM satellite data and raingauge data for microwave applications in Nigeria' *Journal of Atmospheric and Solar-Terrestrial Physics 102, 17–25.*

Ojo J. S,Ajewole M. O and. Olurotimi E. O(2013)" Characterization of Rainfall Structure and attenuation over Two Tropical Stations in Southwestern, Nigeria for the Evaluation of Microwave and Millimeter-wave Communication" *Journal of Meteorology and Climate Science,* Volume 11 (1), 40-48.

Peter, G Fischer, B and Anderson, T (2002): Rain observation with vertically looking Micro rain Radar (MRR), Boreal Environ Res, 7, 353-362.

Peter, G., Fischer, B and Clemens. M (2006): Areal homogeneity of Z-R relations in proceedings of the ERAD 2006.

Rao, T. N., Rao, D.N., Mohan, K and Raghavan, S (2001): Classification of tropical precipitation systems and associated Z-R relationships. J. Geophs Res, 106 (D16), 17699-17711.

Sarmento T. R; Kwon Byung-Hyuk; Silva Moraes Marcia Cristina da (2006): Z-R Relationships for a Weather Radar in the Eastern Coast of Northeastern Brazil, J. Info, Comm and ConvergEng, **4**(1), 42-45.

Sekhon, R.S. and Srivastava, R.C. (1971): Doppler radar observations of drop-size distributions in a thunderstorm. *J.Atmos. Sci.*, **28**, 983–994

Steiner M and Smith, J.A. (2004): A Microphysical Interpretation of Radar Reflectivity–Rain Rate Relationships, *J.Atmos. Sci.*, **61**, 1114–1131.

Strauch, R.G (1976): Theory and applications of FM-CW Doppler radar, Ph.D. Thesis, University of Colorado, 1976

Waldvogel, A. (1974): The *No* Jump of rain drop spectra. *J. Atmos.Sci.*, **31**, 1067-1078.

.

Table

Table 1: Comparison of total number of events and respective events duration of rain type threshold during the study period. Numbers in brackets indicate the total rain accumulation (mm) contributed to the duration based on different rain types.

Threshold of different rain event (mm/h)	$0 < R \leq 5$ Drizzle	$5 < R \leq 10$ Widespread	$10 < R \leq 40$ Shower	$R > 40$ Thunderstorm
Total events	4875	1806	685	291
Events durations (hours)				
Convective (R >10 mm/h)	1789 (80)	1789 (80)	1789 (80)	788 (60)
Stratiform (R ≤ 10 mm/h)	12405 (140)	3523 (100)		
Stratiform and Convective	14194	5312	1789	788

Table 2: Comparison of *Z-R* Relations at different heights (with respective *a* and *b* coefficients and correlation coefficients) andresults from other locations

Rain Types	Source	Location	Z - R	Correlation coefficients
Stratiform Rain	Joss and Gori (1978)	Locarno-mouti	$Z = 250 R^{1.5}$	
	Marshall and Palmer (1948)	Switzerland	$Z=220R^{1.6}$	
	Fujiwara (1965)	Miami, USA	$Z=400R^{1.4}$	
	Ajayi and Olsen (1985)	Ile-Ife, Nigeria	$Z=250R^{1.48}$	
	Present study	**Akure**		
	0-160m		$Z=316R^{1.35}$	
	160-320 m		$Z=249.6R^{1.25}$	
	320-480 m		$Z=249.3R^{1.25}$	0.81
	480-640 m		$Z=252.2R^{1.25}$	0.71
	640-800 m		$Z=250.3R^{1.22}$	0.68
Drizzle	800-960 m		$Z=247.7R^{1.22}$	0.64
	960-1120 m		$Z=244R^{1.21}$	0.76
	1280-1440 m		$Z=239.8R^{1.20}$	0.66
	2720-2880 m		$Z=236.4R^{1.19}$	0.64
	2880-3040 m		$Z=213.2R^{1.15}$	0.65
	Present study			0.80
	0-160 m		$Z=227.1R^{1.18}$	0.73
	160-320 m		$Z=266.8R^{1.19}$	
	320-480 m		$Z=309.5R^{1.12}$	0.58
	480-640 m		$Z=291.7R^{1.11}$	0.53
	640-800 m		$Z=296.9R^{1.09}$	0.50
Widespread	800-960 m		$Z=313.6R^{1.03}$	0.59
	1280-1440 m		$Z=286.9R^{1.05}$	0.60
	1920-2080 m		$Z=190.3R^{1.02}$	0.53
				0.67
				0.66
Convective Rain	Joss and Gori (1978)	Locarno-mouti	$Z = 500 R^{1.5}$	
	Jones (1956)]	Illinois, USA	$Z=486R^{1.37}$	
	Fujiwara (1965)	Miami, USA	$Z=450R^{1.37}$	
	Ajayi and Olsen (1985)	Ile-Ife, Nigeria	$Z=524R^{1.27}$	
Shower	**Present study**	**Akure, Nigeria**		
	0-160 m		$Z=312.5R^{1.1}$	0.64

	160-320 m		$Z=336.9R^{1.1}$	0.58
	800-960 m		$Z=260.7R^{1.1}$	0.52
	960-1120 m		$Z=279.7R^{1.05}$	0.60
	1600-1760 m		$Z=182.1R^{1.18}$	0.75
Thunderstorm	2400-2560 m		$Z=172.8R^{1.07}$	0.69
	Present study			
	0-160m		$Z=380R^{1.06}$	0.86

Table 3: Comparison of *M*-R* relations at different heights (with respective *a* and *b* coefficients and correlation coefficients) and results from other locations

Rain Types	**Source**	**Location**	**M* - R**
Stratiform Rain	Marshall and Palmer (1948)	Switzerland	$M^*=0.072R^{0.88}$
	Ajayi and Olsen (1985)	Ile-Ife, Nigeria	$M^*=0.059R^{0.88}$
Drizzle	**Present study**	**Akure**	
	0-160 m		$M^*=0.078R^{0.7}$
	160-320 m		$M^*=0.09R^{0.65}$
	640-800 m		$M^*=0.079R^{0.86}$
	800-960 m		$M^*=0.078R^{0.89}$
	960-1120 m		$M^*=0.079R^{0.92}$
	1120-1280 m		$M^*=0.079R^{0.93}$
	2720-2880 m		$M^*=0.06R^{0.72}$
	2880-3040 m		$M^*=0.09R^{0.91}$
	Present study		
Widespread	0-160 m		$M^*=0.077R^{0.82}$
	480-640 m		$M^*=0.057R^{0.87}$
	640-800 m		$M^*=0.081R^{0.75}$
	1600-1760 m		$M^*=0.08R^{0.86}$
	1920-2080m		$M^*=0.053R^{0.85}$

Convective Rain	Ajayi and Olsen (1985)	Ile-Ife, Nigeria	$M^{*}=0.063R^{0.89}$
	Sekhon and Srivastava (1971	Cambridge, USA	$M^{*}=0.052R^{0.94}$
	Jones (1956)	Illinois, USA	$M^{*}=0.052R^{0.95}$
	Mueller (1960)	Miami, USA	$M^{*}=0.053R^{0.95}$
Shower	**Present study**	**Akure, Nigeria**	
	0-160 m		$M^{*}=0.067R^{0.93}$
	320-480 m		$M^{*}=0.056R^{0.81}$
	1120-1280 m		$M^{*}=0.063R^{0.87}$
	1440-1600 m		$M^{*}=0.061R^{0.83}$
	1600-1760 m		$M^{*}=0.058R^{0.82}$
	1760-1920 m		$M^{*}=0.067R^{0.84}$
	2880-3040 m		$M^{*}=0.067R^{0.88}$
Thunderstorm	**Present study** 0-160 m		$M^{*}=0.05R^{0.83}$

*M denotes Liquid water content, LWC

FIGURE CAPTIONS

Fig. 1: Vertical profiles spectrum of radar reflectivity obtained by MRR showing the existence of Bright Band (BB) and Non Bright Band (NBB) regions of rain event at(a) 16:20-17:10 GMT LT of 26th October 2010 and (b) 03:40 to 04:50 GMT LT of 31st October 2010.

Fig. 2: Vertical profiles spectrum of different rain parameters obtained by MRR showing no Bright Band (NBB) regions of rain event at 16:55-17:20 GMT LT on 26th October 2010 (a) Radar reflectivity profile (b) rain rate (c) Liquid water content, and (d) average fall velocity.

Fig. 3: Vertical profiles spectrum of different rain parameters obtained by MRR showing the Bright Band (BB) regions of rain event at 16:20-16:30 GMT LT on 26th October 2010 (a) Radar reflectivity profile (b) rain rate (c) Liquid water content, and (d) average fall velocity.

Fig. 4: A typical DSD measured on 26th October 2010 at (a) 160 m (16:20:15 LT) and (b) 640 m (17:10:15LT for different rain events.

Fig. 5: (a) Comparisons of rain rates (b) Scattered plots of MRR rain event with raingauge measurements as observed on the 26th October 2010.

Figures

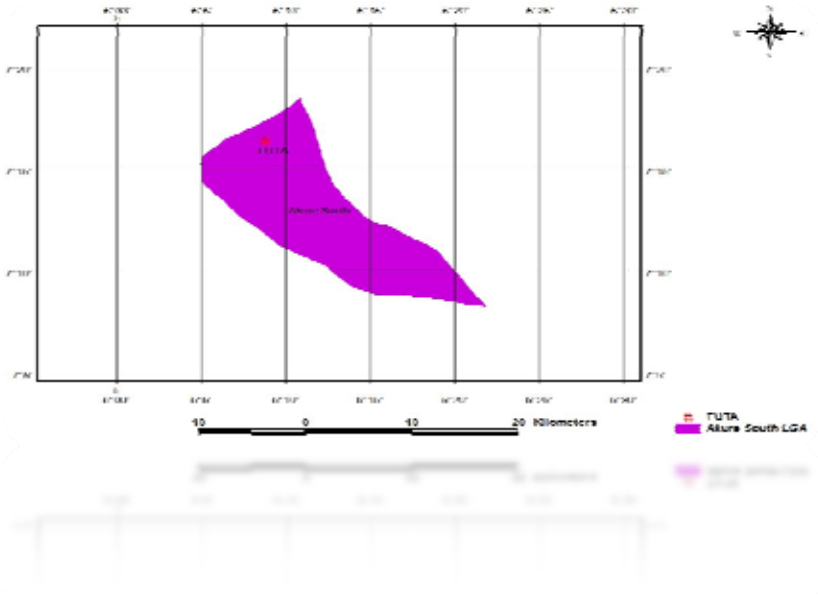

Fig 1: Map of measuring site

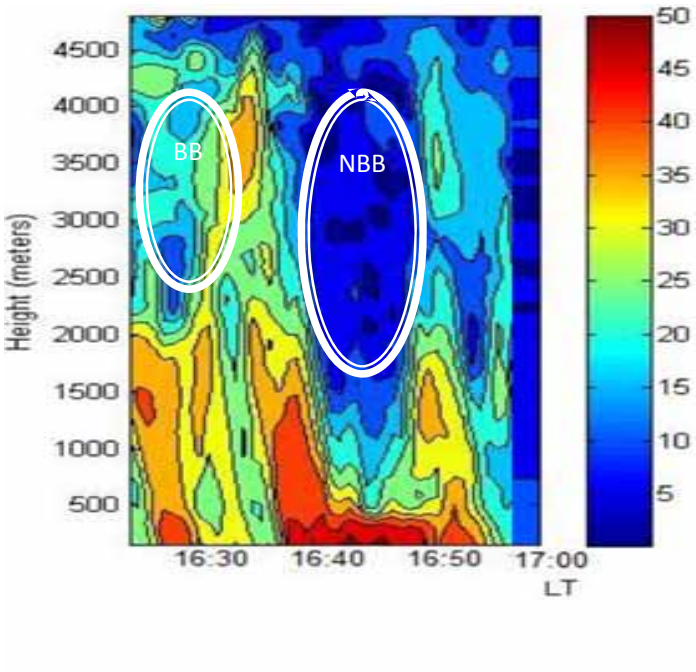
BB
NBB
Height (meters)
4500
4000
3500
3000
2500
2000
1500
1000
500
16:30
16:40
16:50
17:00
LT
50
45
40
35
30
25
20
15
10
5

Fig. 1(a)

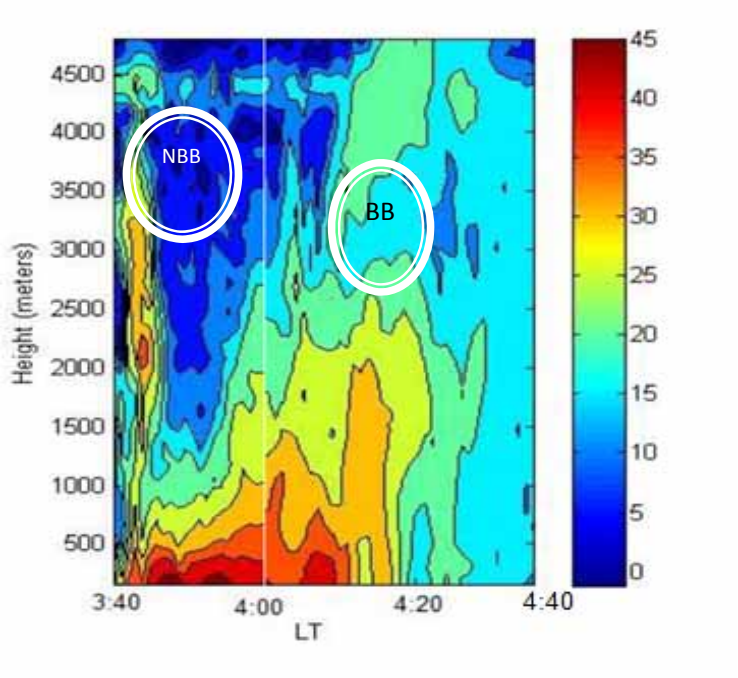
NBB
BB
Height (meters)
4500
4000
3500
3000
2500
2000
1500
1000
500
3:40
4:00
4:20
4:40
LT
45
40
35
30
25
20
15
10
5
0

Fig. 1(b)

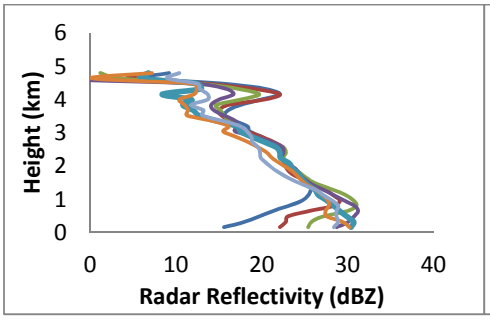

Fig. 2(a)

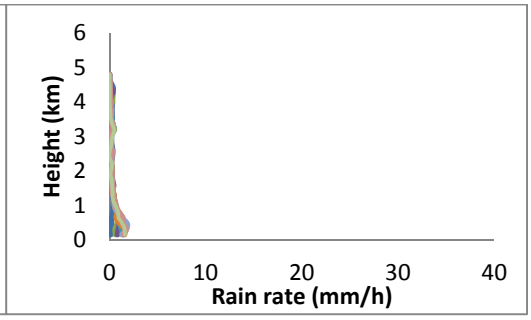

Fig. 2(b)

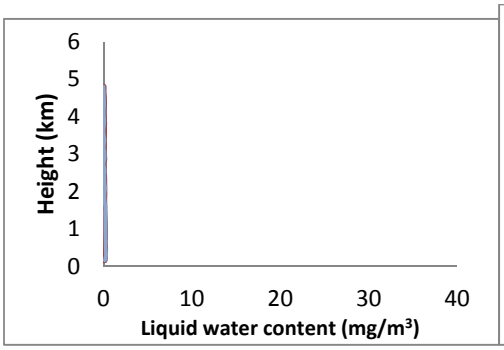

Fig. 2 (c)

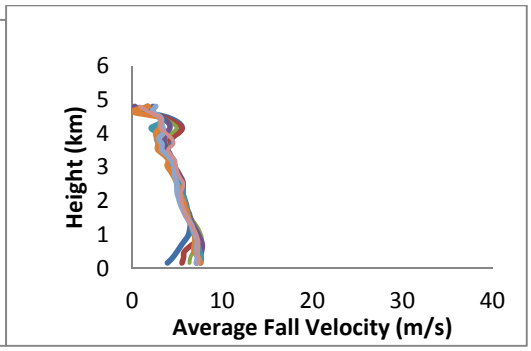

Fig. 2 (d)

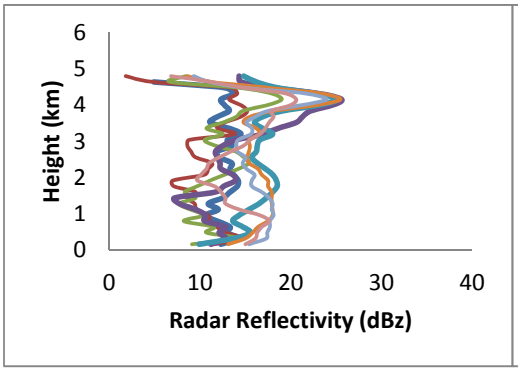

Fig. 3 (a)

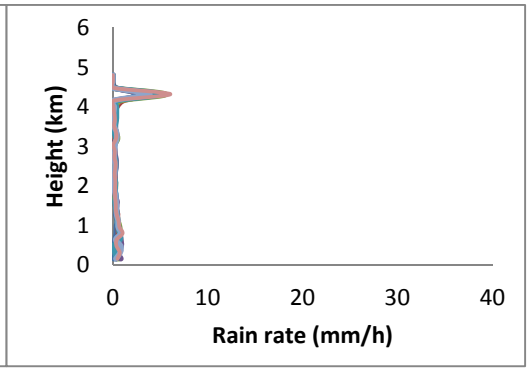

Fig. 3 (b)

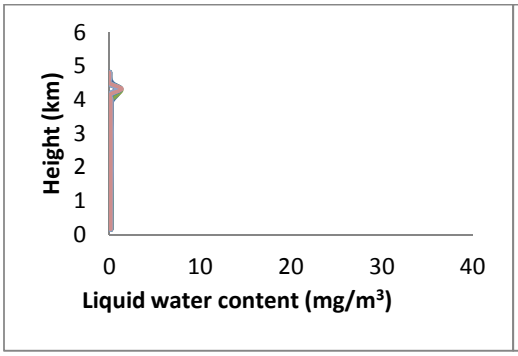

Fig. 3 (c)

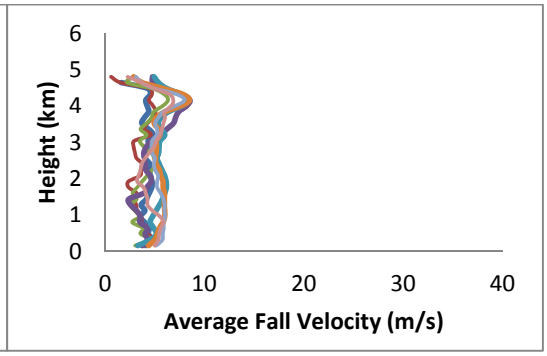

Fig. 3 (d)

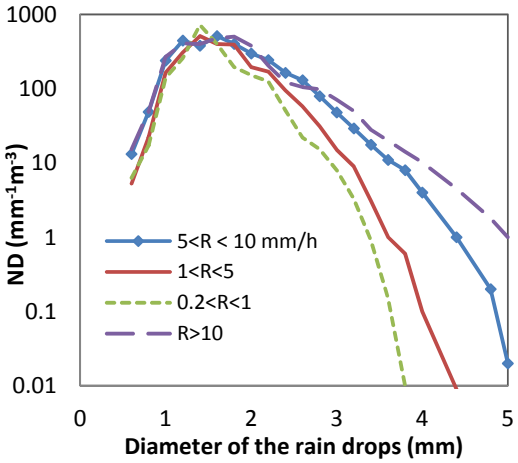

Fig. 4(a)

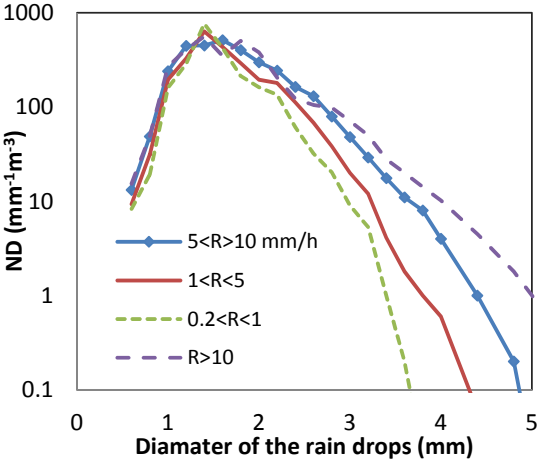

Fig. 4 (b)

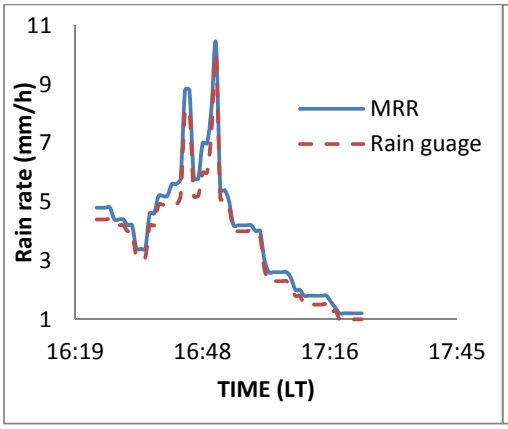

Fig. 5 (a)

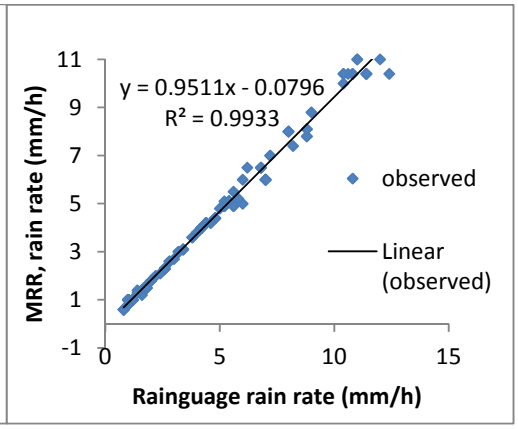

Fig. 5 (b)